

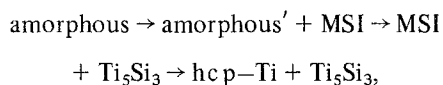
Crystallization characteristics of an amorphous $Ti_{80}Si_{20}$ alloy at high pressures

W. K. WANG*, H. IWASAKI†, C. SURYANARAYANA‡, T. MASUMOTO
The Research Institute for Iron, Steel and Other Metals, Tohoku University, Sendai 980, Japan

Amorphous Ti–20 at % Si alloy, prepared by rapid quenching from the molten state, was annealed while being subjected to a pressure of 10 GPa. X-ray diffraction investigations on the alloy specimens quenched to ambient conditions have shown that pressure greatly alters the crystallization characteristics and a body-centered cubic solid solution having the same composition as that of the parent amorphous matrix forms preferentially at temperatures in the range from 400 to 550° C. The lattice constant of this supersaturated solid solution suggests that silicon atoms are dissolved substitutionally in the titanium lattice. It is not until the temperature is raised to above 550° C that the amorphous matrix decomposes into a bcc solid solution containing less amount of silicon and a silicon-rich phase. Discussion is given on the mode of crystallization on the basis of the present results and those of previous studies and it has been shown that the crystallization of amorphous alloys can be classified into three types depending on pressure and temperature.

1. Introduction

The majority of amorphous alloys studied to date contain either a late transition metal and metalloid or an early transition metal and a late transition metal [1]. A novel class of amorphous alloys will be one containing an early transition metal and a metalloid. Suryanarayana *et al.* [2] succeeded in preparing binary titanium–silicon alloys in the amorphous state by rapid quenching from the liquid state by a melt-spinning technique. They studied by means of electron microscopy and diffraction coupled with differential thermal analysis the transformation behaviour of the amorphous phase to the equilibrium phases and found that the sequence in structural change in this system can be represented as:



where MSI represents a bcc solid solution containing more silicon than the equilibrium terminal solid solution and Ti_5Si_3 an equilibrium intermediate phase having a hexagonal $D8_8$ -type structure.

Iwasaki and his collaborators showed in a series of papers [3–11] that pressure significantly affects the transformation behaviour of amorphous alloys and often leads to the formation of dense, metastable crystalline phases that are not encountered during transformation at ambient pressure. They suggested that, if properly applied, high-pressure annealing of amorphous alloys is a promising method for synthesizing new crystalline phases of multi-component systems [8].

The aim of the present study is to investigate how pressure affects the crystallization behaviour of amorphous titanium–silicon alloys. In this system, the eutectic point is located at the composition of Ti–13.7% Si[§] and the alloys around this

*Present address: Institute of Physics, Chinese Academy of Sciences, P.O. Box 603, Beijing, China.

†To whom all correspondence should be addressed.

‡Present address: Department of Metallurgical Engineering, Banaras Hindu University, Varanasi 221005, India.

§All percentages are expressed in atomic per cent.

composition are most prone to the formation of the amorphous phase [2]. In the present study we have chosen the Ti–20%Si alloy for investigation, which is the alloy with the highest silicon content for the formation of the amorphous phase and is expected to have larger bulk compressibility.

2. Experimental procedures

The Ti–20%Si alloy was prepared from the pure components by arc melting. The amorphous alloy specimens were produced by quenching the molten alloy using a single roller melt-spinning technique where the alloy was levitation melted [12]. About 2 g of the alloys was used per run and the roller speed was about 5000 rpm.

The high pressure apparatus used was the same as that employed in a previous study [13] and hence will not be described here. The amorphous specimens were annealed at temperatures ranging from 350 to 750°C for different periods of time while they were subjected to a pressure of 10 GPa. At the end of the annealing treatment, the a.c. current through the internal heater was shut off and the pressure was then decreased. Crystalline phases, formed during the high-pressure annealing and quenched to ambient conditions, were investigated by X-ray diffraction methods. Since the wavelength of commonly used radiation, $\text{CuK}\alpha$, lay near an absorption edge of titanium, the diffraction pattern was recorded using filtered $\text{MoK}\alpha$ radiation on a flat film placed at a distance of 70 mm from the specimen.

Electron-probe microanalysis (using a Shimadzu EMX-SM) was employed to reveal the distribution of elements in the pressurized specimens.

3. Experimental results

3.1. Transformation at a pressure of 10 GPa

Fig. 1 shows an X-ray diffraction pattern of the Ti–20%Si alloy in the as-melt-quenched state. Only diffuse haloes characteristic of the

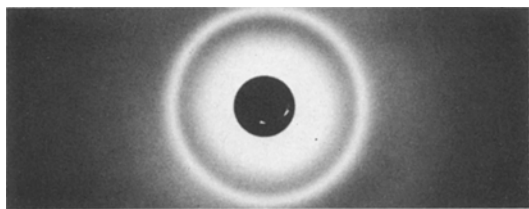


Figure 1 X-ray diffraction pattern of amorphous Ti–20% Si alloy in the as-melt-quenched state. Filtered $\text{MoK}\alpha$ radiation.

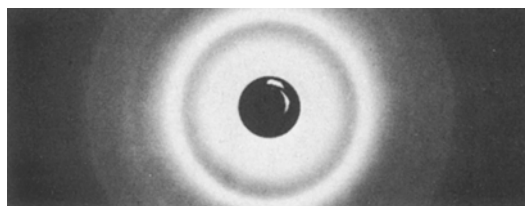


Figure 2 X-ray diffraction pattern of amorphous Ti–20% Si alloy annealed at 10 GPa and 400°C for 30 min, showing the coexistence of the bcc solid solution and the amorphous phase.

amorphous state are seen. Essentially the same diffraction pattern was obtained for the alloy annealed at 10 GPa and 360°C for 800 min, indicating that the amorphous phase remained unchanged upon such low-temperature annealing. A change in the diffraction pattern is seen if the temperature of annealing is raised to 400°C, as shown in Fig. 2. Although the haloes still remain, several weak diffraction lines appear which can be identified as those arising from the bcc structure. However, this bcc phase has significantly different lattice constant from that of MSI forming from the amorphous matrix at ambient pressure. This becomes more evident when the annealing temperature is further raised. Fig. 3 shows an X-ray diffraction pattern of the alloy annealed at 10 GPa and 500°C for 15 min. Diffuse haloes have disappeared and diffraction lines from the bcc structure are now clearly seen, from which the lattice constant is measured to be $a = 0.3168 \pm 0.0007$ nm, considerably smaller than that of MSI, $a = 0.32$ nm [2]. The lattice constant of bcc pure titanium, estimated by an extrapolation to 25°C of the values at high temperatures using the linear expansion coefficient [14], is 0.3276 nm. The smaller atomic size of silicon compared with that

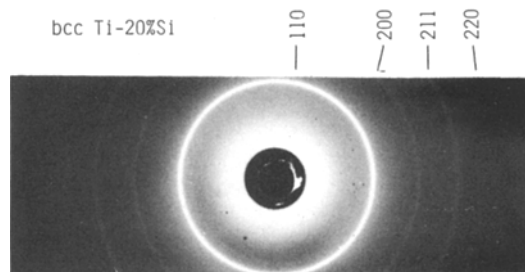


Figure 3 X-ray diffraction pattern of amorphous Ti–20% Si alloy annealed at 10 GPa and 500°C for 15 min, showing complete transformation into the bcc solid solution (SSS).

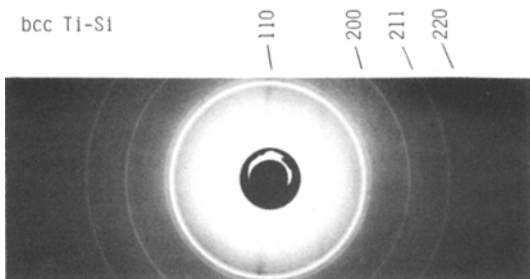


Figure 4 X-ray diffraction pattern of amorphous Ti-20% Si alloy annealed at 10 GPa and 750°C for 3400 min, showing decomposition into depleted bcc solid solution and X phase.

of titanium suggests that the bcc phase formed at high pressure is a substitutional solid solution of silicon in titanium. The MSI phase formed at ambient pressure is also a substitutional solid solution, but it contains a lesser amount of silicon. As will be shown below, no indication of enrichment or depletion of a particular element is observed in the alloy specimen containing the high pressure bcc phase and, therefore, this phase with the smaller lattice constant is undoubtedly a product of direct transformation of the amorphous phase

without any decomposition. It is hereafter called SSS (supersaturated solid solution). SSS forms in the compressed alloy in a wide range of temperature, from about 400 to 550°C, and it remains unchanged upon annealing for as long as 2000 min. Annealing at higher temperatures results in the formation of a two-phase mixture of another bcc phase and a complex phase, called X phase. This is unambiguously seen in an X-ray diffraction pattern of Ti-20% Si alloy annealed at 10 GPa and 750°C for 3400 min shown in Fig. 4. The lattice constant of this bcc phase, 0.3207 ± 0.0006 nm, is larger than that of SSS, indicating that it contains a smaller amount of silicon and corresponds to MSI. The decrease in silicon content is due to the formation of the X phase, which is not identified but must be rich in silicon content.

Time-temperature-transformation diagram of amorphous Ti-20% Si alloy at a pressure of 10 GPa has been constructed and is shown in Fig. 5. As compared with the transformation characteristics of the alloy at ambient pressure [2], two notable differences can be observed. Firstly, the crystallization temperature, defined as the location of the boundary between the amorphous region

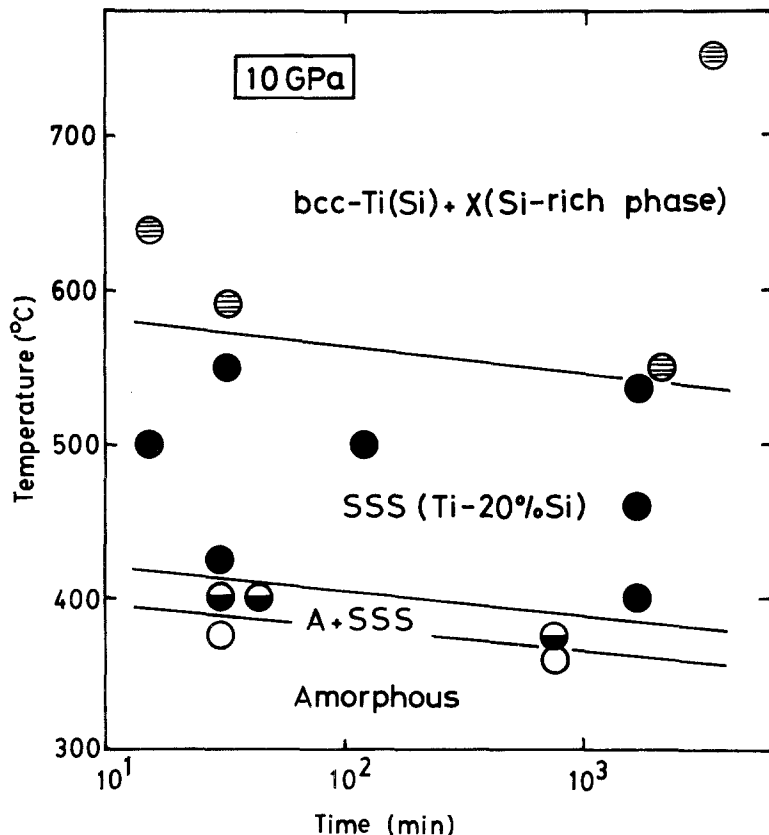


Figure 5 Time-temperature-transformation diagram of amorphous Ti-20% Si alloy on annealing at 10 GPa.

and the amorphous + SSS region in the diagram, is not much different from the temperature, 430°C, at which MSI forms at ambient pressure. This makes a striking contrast to the crystallization of amorphous Pd–20% Si [3], Fe–17% B [4] and Nb–19% Si [9] alloys, for which pressure appreciably raises the crystallization temperature. Secondly, formation of the hcp-titanium and Ti₅Si₃ phases is suppressed at high pressure. At ambient pressure, annealing at higher temperatures, 545°C for 60 min or 700°C for 1440 min, brings the alloy into the two-phase state of hcp-Ti and Ti₅Si₃ [2], while, at 10 GPa, annealing at a temperature as high as 750°C does not lead to the formation of hcp-Ti (nor hcp solid solution of titanium and silicon).

3.2. Distribution of constituent elements in the Ti–20% Si alloy

Using the same alloy specimens as those for the X-ray diffraction examination, electron-probe microanalysis was carried out to investigate a change in distribution of constituent elements associated with the structural change. Fig. 6a is the scanning curves, obtained using TiK α and SiK α characteristic radiation, across the surface of the amorphous specimen before annealing. It shows the homogeneous distribution in the alloy, as expected. The scanning curves of the alloy specimen annealed at 10 GPa and 400°C for 30 min are shown in Fig. 6b. This specimen contains SSS embedded in the remaining amorphous matrix, but the curves are essentially the same in the form as those of the homogeneous amorphous specimen, indicating that there is no composition fluctuation even when SSS forms. Evidence of heterogeneity appears after the amorphous phase is transformed into a mixture of the bcc and X phases, as seen in Fig. 6c. The curves shown there were obtained from the alloy specimen annealed at 10 GPa and 750°C for 3400 min and the intensity of TiK α and SiK α radiation, though apparently not complementary to each other due to absorption effects, fluctuates from place to place appreciably. These observations show unequivocally that pressure suppresses composition fluctuations which might otherwise occur in the amorphous phase and leads to the formation of a crystalline phase having the same solute content as that of the parent amorphous phase. It is not until the temperature is raised considerably that crystallization accompanied by composition change takes place.

4. Discussion

4.1. Effect of high pressure on the crystallization of amorphous alloys

We have observed the formation of SSS or bcc-Ti(Si) + X depending on the annealing temperature in the pressurized amorphous Ti–20% Si alloy. In previous studies [3–11], different kinds of crystalline phases were observed in different kinds of pressurized amorphous alloys. We are now in a position to deduce a unified picture of the crystallization behaviours at high pressure.

It is possible to classify the behaviours into three distinct types. One of them involves decomposition of amorphous phase into crystalline phases having different solute contents, as in Pd–20% Si [3], Fe–17% B [4], Fe–13% P–7% C [10] and Co–20% B [10] alloys. These alloys are decomposed into a mixture of respective mother metal and intermetallic compound, whose structure is not necessarily the same as that in an equilibrium state at ambient pressures. This type of crystallization is also observed for Nb–19% Si alloy [9] and the present Ti–20% Si alloy when they are annealed at higher temperatures. In all of these alloys the crystallization under pressure sets in at temperatures higher than those at ambient pressure. The second type involves the formation of ordered crystalline phases such as the A15 phase in Nb–19% Si [9] and Nb–23.7% Si [8, 11] alloys, the DO_e phase in Fe–20% B alloy [10]. These crystalline phases are almost homogeneous in the respective alloys, i.e. exist in a single-phased state, and therefore each has a composition not different from that of the parent amorphous phase. The third type involves the formation of a single-phased solid solution having no long-range order in atomic arrangements. This type of crystallization is found in the present Ti–20% Si alloy (formation of SSS). If the magnitude of pressure is greatly increased by using a shock compression technique, the second type of crystallization preferentially occurs in the alloy for which the first type of crystallization has been observed. This is the case with Co–20% B alloy (formation of the DO₁₁ phase) [10]. Switching of the type also occurs in Nb–22% Si alloy [6] and shock compression induces a transformation of amorphous phase into a supersaturated fcc solid solution. Fig. 7 schematically depicts the three types of crystallization in amorphous alloys.

What are the factors which control the type of crystallization? The first type occurs when the

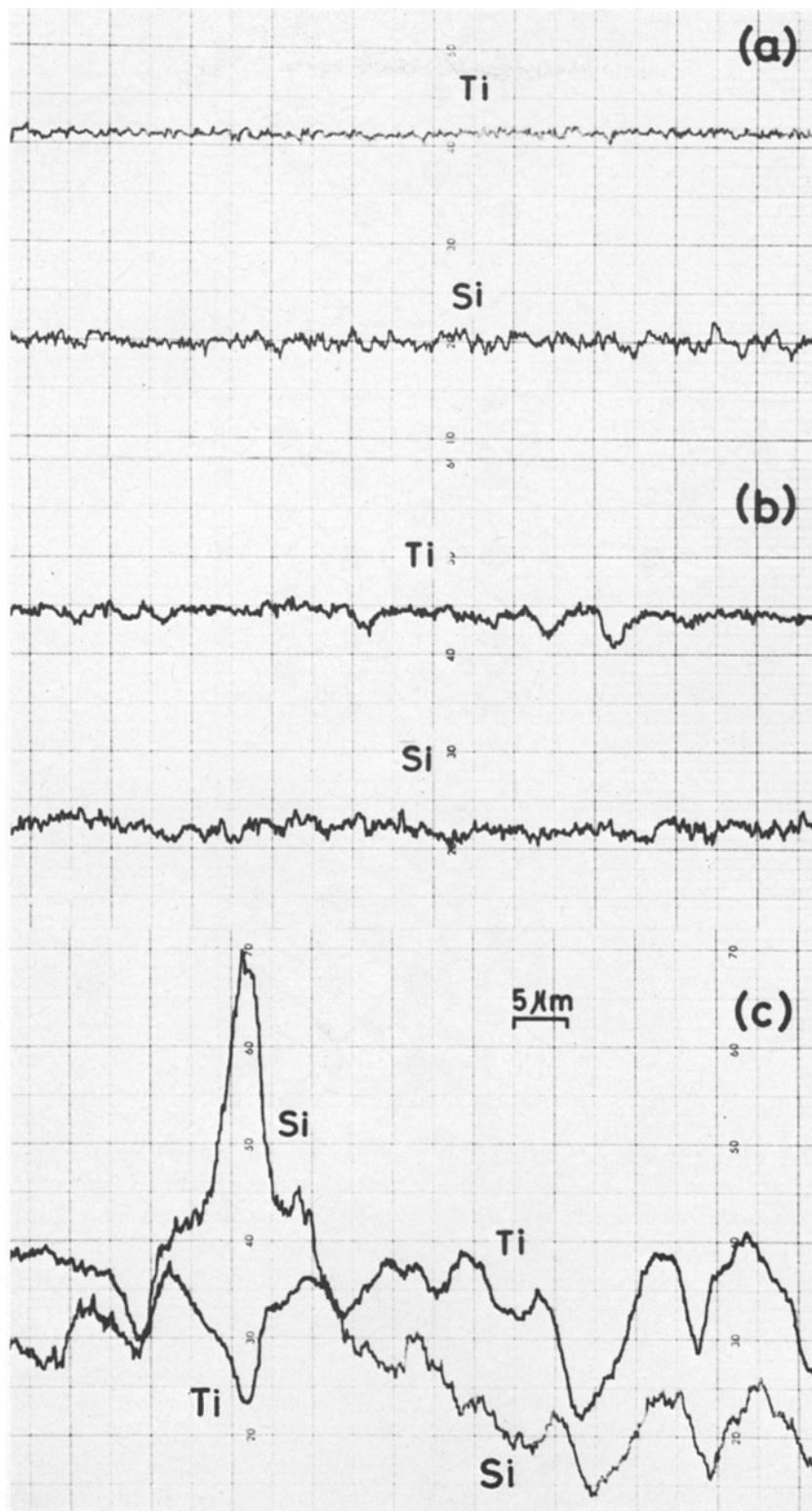


Figure 6 Electron-probe scanning curve of Ti–20% Si alloy recorded using $TiK\alpha$ and $SiK\alpha$ radiation. (a) in the as-melt-quenched state, (b) after annealing at 10 GPa and 400°C for 30 min and (c) after annealing at 10 GPa and 750°C for 3400 min.

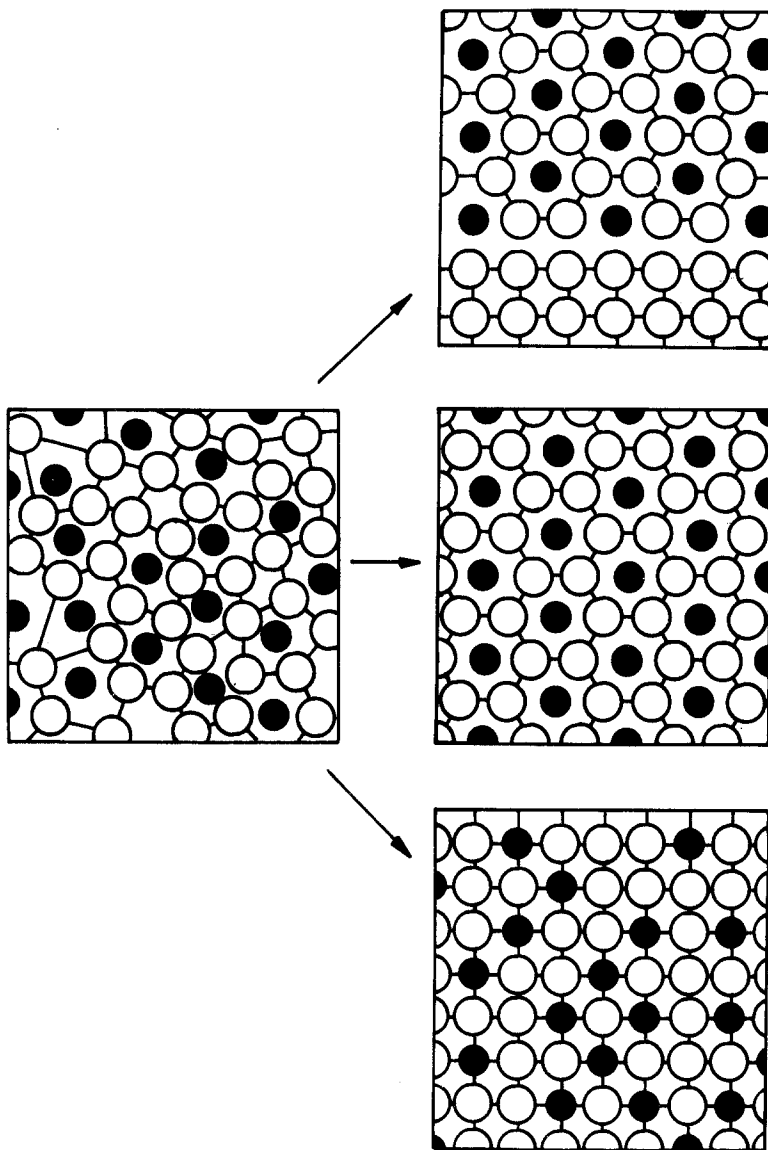


Figure 7 Pictures illustrating the three types of crystallization of amorphous alloys under high pressure. Left, amorphous phase. Right; top, decomposition into a mixture of phases, middle, transformation into an intermetallic compound, bottom, transformation into a supersaturated solid solution.

reduction of alloy volume is relatively small and/or the temperature of annealing is high. The compressibility data of the above mentioned alloys are not available, but it is not unreasonable to assume that the alloys based on iron, cobalt and palladium are less compressible whereas those based on titanium and niobium are compressible. The compressibilities reported for the elemental materials here concerned [15] lend support to the assumption, except for niobium. The crystallization of the first type is essentially the same as the crystallization of amorphous alloys at ambient pressure. Since atomic diffusion is involved in this transformation, reduction of volume results in an increase in the height of potential barrier across which atoms move and hence the crystallization temperature is

shifted towards higher temperature with the application of pressure. Even if the reduction of volume is large, the decomposition type (first type) crystallization can occur at temperatures high enough to allow diffusion of atoms, as observed on high temperature annealing of the compressed Nb-19% Si and Ti-20% Si alloys. When the reduction of volume becomes large while the temperature of annealing is kept to be low, crystallization of the second or third type (non-decomposition type) occurs, in which diffusion of atoms over long distance is not involved and the amorphous phase yields to compressive forces by forming periodic dense-packed structure with minimum rearrangement of atoms. This type of crystallization has some resemblance to the pressure-induced

crystallization of amorphous elemental materials such as silicon, germanium, arsenic, etc. The crystallization temperature is hardly affected by the application of pressure and in some cases the transformation into the crystalline state starts at temperatures lower than the crystallization temperature observed at ambient pressure [6]. Which kind of crystalline phase, intermetallic compound or supersaturated solid solution, compressed amorphous phase prefers is dependent on the alloy composition as well as on the factors such as atomic size ratio, electronegativity difference between component atoms, etc. Pressure can also have an influence and the solid solution is formed under heavier compression, as observed for Nb–22% Si alloy.

Titanium metal has two modifications at ambient pressure: the bcc form is stable at temperatures higher than 880°C and the hcp form at temperatures below. The structural change from MSI having the bcc structure into the terminal solid solution having hcp structure observed upon prolonged annealing (at 545°C or 700°C) of the amorphous Ti–20% Si alloy at this pressure is understood in terms of the approach to a more stable state. The results of the present study show that pressure prevents transformation of the bcc structure formed from the amorphous matrix into the hcp form even at a temperature as high as 750°C. This is presumably due to an increased stability of the bcc structure compared with the hcp structure at high pressure. Crystallographic data of titanium metal shows that the axial ratio c/a of the hcp form deviates considerably from the ideal value 1.633 and the density increases by 2.84% upon transformation from the hcp form to the bcc form [16]. The fact that the application of pressure shifts the transition temperature between the hcp and bcc forms towards lower temperatures [17] is a natural result of this increase. If the same situation holds for the Ti–Si solid solution, the bcc form is more stable than the hcp form under pressure.

4.2. Calculation of the lattice constant of SSS on the basis of a pair-potential model

We have obtained the value 0.3168 nm as the lattice constant of SSS, the bcc Ti–20% Si solid solution. The maximum solid solubility of silicon in bcc titanium at ambient pressure was reported to be 5% [18], but there are no lattice constant

data for the bcc Ti–Si solid solution. As mentioned above, SSS is of the substitutional type and a Vegard's law calculated using the atomic diameter for $CN = 8$ of 0.2535 nm for silicon [19] yields $a = 0.3209$ nm for Ti–20% Si alloy, considerably larger than the observed value. An attempt is made here to calculate the lattice constant employing a more realistic model of solid solution. Machlin [20] proposed a pair potential model in order to predict the lattice constant of substitutional solid solution. In this model, total energy of the solid solution is given as a sum of pairwise interactions between constituent atoms and an equilibrium lattice constant is obtained by minimizing the total energy. Due account is taken for electron transfer between atoms having different electronegativity. Parameters required for the calculation are the atomic diameter of titanium and silicon for $CN = 8$, their electronegativity, screening constant and bulk cohesive energy of titanium and silicon in the bcc form. The values used are taken from Machlin's paper [19, 21] and listed below.

	Ti	Si
atomic diameter (nm)	0.284	0.2535
electronegativity	1.4	1.9
screening constant	0.5	0.25
cohesive energy (kJ mol ⁻¹)	471.5	426.3

The constant a included in the formula defining the effective atomic diameter is put to be 0.75, following the suggestion given by Machlin. The pair potential model then yields a value of 0.3188 nm for the lattice constant of the bcc Ti–20% Si solid solution (SSS). An improvement is achieved, showing that the model can be used extensively to predict the lattice constant of supersaturated solid solutions to be produced by the high-pressure annealing of amorphous specimens in other alloy systems.

Acknowledgements

Two of the present authors (WKW and HI) wish to express thanks to Professor He of Institute of Physics, Chinese Academy of Sciences, for his interest in the present work. It has partly been supported by the fund from the Mitsubishi Foundation.

References

1. C. SURYANARAYANA, "Rapidly Quenched Metals – A Bibliography 1973–1979" (IFI/Plenum,

- New York, 1980).
2. C. SURYANARAYANA, A. INOUE and T. MASUMOTO, *J. Mater. Sci.* **15** (1980) 1993.
 3. H. IWASAKI and T. MASUMOTO, *ibid.* **13** (1978) 2171.
 4. W. K. WANG, H. IWASAKI and K. FUKAMICHI, *ibid.* **15** (1980) 2701.
 6. W. K. WANG, Y. SYONO, T. GOTO, H. IWASAKI, A. INOUE and T. MASUMOTO, *Scripta Metall.* **15** (1981) 1313.
 7. W. K. WANG, H. IWASAKI, C. SURYANARAYANA, T. MASUMOTO, K. FUKAMICHI, Y. SYONO and T. GOTO, in Proceedings of 4th International Conference Rapidly Quenched Metals, Sendai, August 1981, edited by T. Masumoto and K. Suzuki (The Japan Institute of Metals, Sendai, 1982) p. 663.
 8. H. IWASAKI, W. K. WANG, N. TOYOTA, T. FUKASE, H. FUJIMORI, Y. AKAHAMA and S. ENDO, *Solid State Commun.* **42** (1982) 381.
 9. W. K. WANG, H. IWASAKI, C. SURYANARAYANA, T. MASUMOTO, N. TOYOTA, T. FUKASE and F. KOGIKU, *J. Mater. Sci.* **17** (1982) 1523.
 10. W. K. WANG, Thesis, Tohoku University (1982).
 11. H. IWASAKI, *Sci. Rep. RITU A31* (1983) 1.
 12. A. INOUE, S. SAKAI, H. M. KIMURA and T. MASUMOTO, *Trans. Jpn. Inst. Met* **20** (1979) 255.
 13. H. IWASAKI, Y. WATANABE and S. OGAWA, *J. Appl. Crystallogr.* **7** (1974) 611.
 14. W. B. PEARSON, "A Handbook of Lattice Spacings and Structures of Metals and Alloys", Vol. 2 (Pergamon Press, Oxford, 1967) p. 1279.
 15. J. N. PLENDEL and P. J. GIELISSE, *Phys. Status solidi* **42** (1970) 681.
 16. H. W. KING, in "Alloying Behaviour and Effects in Concentrated Solid Solutions", edited by T. B. Massalski (Gordon and Breach, New York, 1965) p.85.
 17. W. KLEMENT JR and A. JAYARAMAN, in "Progress in Solid State Chemistry", Vol. 3, edited by H. Reiss (Pergamon Press, Oxford, 1967) p. 316.
 18. M. HANSEN, "Constitution of Binary Alloys" 2nd edn-(McGraw-Hill, New York, 1958) p. 1198.
 19. E. S. MACHLIN and S. H. WHANG, *J. Phys. Chem. Solids* **37** (1976) 555.
 20. E. S. MACHLIN, *Acta Metall.* **24** (1976) 543.
 21. *Idem, ibid.* **22** (1974) 95.

*Received 13 April
and accepted 26 April 1983*